IEEE Access
Multidisciplinary ⋮ Rapid Review ⋮ Open Access Journal

Date of publication xxxx 00, 0000, date of current version xxxx 00, 0000.

Digital Object Identifier 10.1109/ACCESS.2023.0322000

Optimal Infrastructure Design and Power Management for a Photovoltaic and Battery Assisted Electric Vehicle Charging Station in Southern California

YU YANG[1], HEN-GEUL YEH[2] (Senior Member, IEEE), and Nguyen Cam Thuy Dam[1]
[1]Department of Chemical Engineering, California State University Long Beach, Long Beach, CA 90840 USA (e-mail: yu.yang@csulb.edu)
[2]Department of Electrical Engineering, California State University Long Beach, Long Beach, CA 90840 USA (e-mail: Henry.yeh@csulb.edu)

Corresponding author: Hen-Geul Yeh (e-mail: Henry.yeh@csulb.edu).

This work is supported by the State of California SB1 through the Trustees of the California State University (Agreement #ZSB12017-SJAUX) and the California State University Transportation Consortium.

ABSTRACT This paper presents a framework for the optimal design of a solar and battery assisted electric vehicle (EV) charging station in southern California, with a focus on maximizing long-term profits while addressing operational uncertainties. The problem is conceptualized as an iterative two-stage decision process. In Stage I, the sampled designs of station infrastructure, including the number of chargers, the size of photovoltaic (PV) array, and capacity of the battery energy storage system (BESS), are specified. In Stage II, the charging rule is designed and simulated based on the charging request and solar power datasets. A model predictive controller and an empirical rule-based approach with incoming car forecasts are developed and compared for the vehicle charging management. The simulated annual operational profit and infrastructure investment with the consideration of long-term battery degradation is synthesized to build response surface for better design exploration in Stage I. We find that the proposed rule-based approach is computationally more efficient and suitable to integrate with response surface methodology (RSM) for design optimization. In addition, RSM is compared with adaptive particle swarm optimization (PSO) with multiple trials to demonstrate its superiority in high-profit design.

INDEX TERMS Battery energy storage system, model predictive control, photovoltaic systems, response surface methodology

List of Symbols

α_B	Battery cost
α_C	Charging service fee per kWh
α_G	Grid TOU price
α_S	Solar power incentive per kWh
β	Remained battery energy
Δ	Decision time interval, 15 minutes
$\eta_l(h)$	Required energy at spot l, time h
$\hat{\mathcal{R}}_H$	H-step predicted operational revenue
λ	Level distance in RSM
$\mathcal{P}$	10-year profit
$\mathcal{R}$	Annual operational revenue
ν	Open spots in the charging station
$\overline{\gamma}$	Charging requests prediction
$\Theta(h)$	Set of occupied charging spots at time h
$\tilde{\mathcal{R}}$	Approximated annual operational revenue
B	Battery size
b	Battery charging/discharging power
H	MPC prediction horizon
h	Time instant
L	Level changing diection in RSM
l	Charging spot index
M	The maximum solar power generation
N	Number of chargers
P	PV capacity
p^c	EV power consumption
p^g	Solar power generation
$p^{g'}$	Non-grid power source
Q	Maximum power output, 7.2, 11 or 22 kW
$T_l(h)$	Allowable waiting time at spot l, time h
$T_{h\to 6}$	Duration from time instant h to 6 AM
$x_l(h)$	Charging power at spot l, time h

I. INTRODUCTION

As CO_2 and air pollution continuously attract worldwide attention, electrical vehicles (EV) are emerging as a promising alternative to fossil fuel vehicles in the transportation sector due to its zero emission nature. Nevertheless, this transition process faces numerous challenges and may require a significantly long period. For instance, the California government has set an ambitious target of having 5 million zero-emission vehicles (ZEV) on the road by 2030, but only 862,874 cumulative ZEV sales has been realized through the first quarter of 2021 [1]. One of the significant hindrances to widespread EV adoption in daily transportation is the insufficiency of public charging infrastructure [2]. In California, 70,000 public and shared chargers were installed by Jan 2021, yet an estimated 700,000 chargers are needed to accommodate 5 million ZEV on road [1]. This disparity underscores the urgency for collaborative efforts among government, industry practitioners, and academia to collaborate and work out an economically viable solution for the development of charging stations.

One of the most important factors to impact the operating cost of a charging station is its power supply. Although the grid is a traditional power source for charging stations, as the efficiency of photovoltaic (PV) cells increases, the integration of charging stations and PV farms will be economically more efficient. In addition, when a large number of EVs are connected to the grid, the resulting high power demand will incur significant drop on service quality and safety issues [3], [4]. Hence, on-site solar power can be an alternative choice for EV charging station to enhance its grid independence. However, the intermittent nature of solar power may introduce considerable fluctuations in the power supply, and thus battery energy storage systems (BESS) are recommended to couple with solar panels in the charging station design. Both battery and solar panels are capital-intensive investments, and thereby their optimal size to generate maximum profit will be the research focus of this paper. Besides, given the specific capacity of battery and solar panels, the EV charging policy and number of plugs will also impact the financial status and operations of a charging station, which deserve more investigations.

The charging station infrastructure design can be formulated as an optimization problem. In [5], the charging station design, without PV and battery, is cast as a two-stage stochastic program with only 28 scenarios to develop charging profiles with very limited uncertainties and duration. In [6], energy usage, electricity cost, weather, geographic location, inflation, and battery aging are considered to minimize the long-term overall cost. The resulting mixed-integer nonlinear program (MINLP) is solved over the entire life cycle of PV panels and BESS. In [7], the battery size and daily charging profile are determined simultaneously to minimize the cost by solving a mixed integer linear program (MILP). However, the charging demand in [7] is modeled as a probability function derived from a general database. A similar work highly relying on solar and demand predictions is proposed in [8] by solving a MILP and its convex relaxation to determine the daily charging profile and battery size. In [9], different combinations of renewable energy systems are enumerated to determine the lowest overall system cost. Such calculations are conducted through the software HOMER, developed by the National Renewable Energy Laboratory (NREL). Because the optimal sizing of infrastructure may involve complex models, constraints, and non-differential terms, [10] uses the differential evolution (DE) algorithm to optimize multiple-objectives, including power loss, charging cost, and voltage stability, simultaneously. Reference [11] uses genetic algorithm-particle swarm optimization (GA-PSO) hybrid approach to solve the similar multi-objective optimization for charging stations siting and sizing. Reference [12] employs a similar multi-objective optimization method for charging station design with aging battery and PV. That work only simulates 5 days operations, which could be far from the real charging performance. These metaheuristic methods may need to enumerate a large number of solutions and repeat with many trials. The response surface methodology (RSM) builds the relationship of inputs and response variables through carefully designed sampling schemes. For example, the Box-Behnken (BB) design only needs 13 initial samples to construct the response surface for any 3-variable problem [13]. Then, the search space can be gradually reduced to reach a near-optimal solution. In summary, the existing methods try to formulate the design problem as a large-scale MINLP/MILP, whose complexity increases significantly as the long-term charging operations and uncertainties are considered. The optimization method adopted by these literature, such as PSO or GA, may not be efficient enough to find an optimal design.

Given a specific station infrastructure, the EV charging policy should be designed to meet customers' demands and maximize the operational revenue. The charging operation design can be categorized into centralized and decentralized approaches. Centralized approaches gather and analyze data from all EVs and the power grid to determine the optimal charging operations for each customer, while decentralized approaches allow each EV to decide its charging power solely based on its own status [14]. The centralized approaches need more computation and communication resources, but its solutions can be more profitable. Limmer [15] demonstrates that a centralized optimization-based charging approach is better than equally power dispatching to each EV. In [16], a centralized convex optimization formula is proposed for the charging and discharging schedule. When the PV power system is integrated with charging stations, the power dispatch policy can be more flexible. Kabir et al. [17] study purely using PV-generated energy for charging and assess the significance of solar power and upcoming EV load predictions. Nevertheless, this centralized method takes a long time to reach an optimal solution. Tushar et al. [18] classify EVs into three types and design their daily charging policies via MILP offline to reduce the intermittency of electricity supply and facilitate the cost reduction of PV-powered charging stations. In [19], [20], the PV-assisted EV-charging schedule problem is modeled as a Markov decision process (MDP) to minimize the average

waiting time of EVs under the long-term cost constraint. The MDP can then be solved by reinforcement learning offline to shorten the online decision-making time. Yan et al. [21] develop a two-stage optimization formula to allocate power source and then dispatch the power to each connected EV. Ghotge et al. [22] employ model predictive control (MPC) for charging policy design on a PV-assisted parking lot under EV arrival and demand uncertainties. They also find that the forecasting of EV energy demands can significantly affect the charging station and power grid performances. Zhang et al. [23] design a dynamic charging scheduling scheme that uses MPC and real-time information to schedule EV charging to maximize the operational profit of the station. Similar to MPC, a moving horizon optimization framework has been developed with several objective functions including the cost minimization and valley filling [24]. Zheng et al. [25] show that the fuzzy rule can be integrated with distributed MPC to minimize the charging cost with the consideration of power flow model. In summary, existing charging management methods heavily rely on the real time optimization, but are hard to be integrated into design formulas due to their high computational burdens.

We propose a response surface based charging station design method combined with EVs charging power management. The study data is gathered from an EV parking lot in our university. We analyze the real data, encompassing variables like charging energy demands, permissible waiting times, and solar power generation, to design and compare MPC and empirical rule based charging strategies given the same infrastructure. MPC relies on the hour ahead solar power and 15-minute ahead incoming car number forecast to assign the charging power for individual EV at each time instant. It repeatedly maximizes the operational revenue over the prediction time frame in a receding horizon fashion, with the consideration of time of use (TOU) price and BESS operations. In addition, an empirical rule is also designed solely based on 15-minute ahead incoming car number forecast to determine on-spot EV charging power. A charging demand peak occurs around 4 PM because of the university course schedule. During that period, solar energy is not rich and TOU price is high. The BESS charged by solar energy provides power to EVs after 4 PM instead of using grid power with a high price. The charging order is decided based on the energy demand and waiting time. Utilizing the rule-based method or MPC, various design combinations are efficiently enumerated to obtain the resulting annual revenue. Subsequently, the ten-year overall profit is computed by considering both operating revenue and capital investment. This comprehensive assessment aids in determining the optimal BESS capacity, PV size, and number of chargers. Even though integrating charging operation with infrastructure design has been considered very recently [26], that approach combines total EVs energy demand as a single variable for annual operation design to reduce the computational burden, which may deviate from realistic operations.

In contrast to references and our preliminary results [27], the new contributions are summarized below:

(i) The MPC and empirical rule-based charging strategies are designed with various prediction models. Our findings show that an empirically designed rule-based charging schedule with incoming car prediction leads to slightly lower profit than the MPC, but significantly reduces the computational time because online optimization is not required.

(ii) A RSM scheme is developed to size BESS capacity, charger numbers, and solar panel capacity, while optimizing the 10-year pay back. The rule-based charging strategy allows for the simulation of practical one-year operations, which provide annual revenue for infrastructure design. Furthermore, the RSM can take the battery capacity degradation into account to achieve more realistic solutions. To our best knowledge, this paper is among the first to consider detailed annual operations in station design and we demonstrate that RSM is more efficient than some standard intelligent optimization methods, such as PSO.

The rest of this article is organized as follows. Section II presents the case description. Section III shows the charging power management approaches, including MPC and empirical rule. In Section IV, the RSM is proposed to determine the quantity of chargers, capacity of solar panel, and size of BESS. In Section V, the charging profiles and resulting profits under various infrastructure sizes are demonstrated for comparison. Finally, the conclusion is drawn in Section VI.

II. CASE DESCRIPTION

An EV charging station on our campus combined with a solar farm is investigated. The J1772 type-I charger, with quantity N and power limit Q kW, are employed. Here Q can be 7.2, 11, or 22. The PV power capacity is denoted as P. A BYD lithium iron phosphate BESS is equipped, whose capacity is denoted as B. α_B denotes the capacity-dependent BESS cost. The charging service mainly relies on solar energy or battery, and its power demand gap is covered by the grid. The TOU price is considered in this study, denoted as α_G. The charging service fee is flat α_C =\$0.40/kWh. Besides the charging service, the net surplus compensation rate for solar power is assumed to be α_S =\$0.04/kWh [30]. The objective of this research is to determine the number of deployed chargers N, battery capacity B, PV capacity P, and a charging policy to maximize the 10-year economic profit of this charging station.

The California Solar Initiative (CSI) 15-minute interval power generation data gathered at a nearby airport, with the distance to campus less than 3 miles, is used to simulate the solar energy profile [31]. This study assumes the capacity factor of commercial PV to be 19.1%, and sampled power profiles per unit in January are shown in Fig. 1. Additionally, the charging data including the details of arrival time, allowed duration, and energy demand on our university campus is collected and used in the simulation. A typical energy request profile on a weekday is shown in Fig. 2. The highest charging peak occurs around 8 AM (time instant 32) due to the morning class schedule. In addition, several charging requests were

received after 4 PM (time instant 64) because of the evening class schedule.

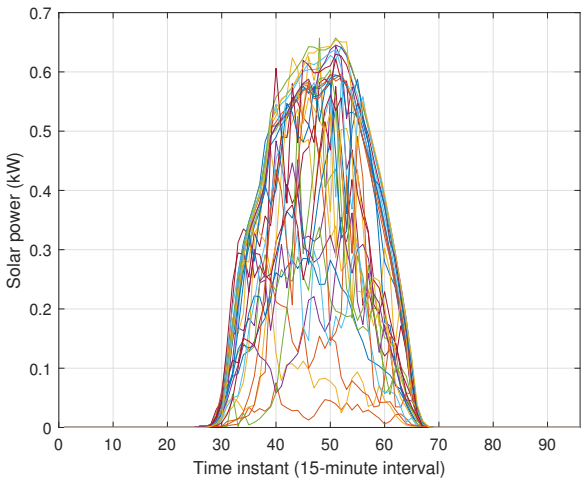

FIGURE 1. Solar power generation baseline in January.

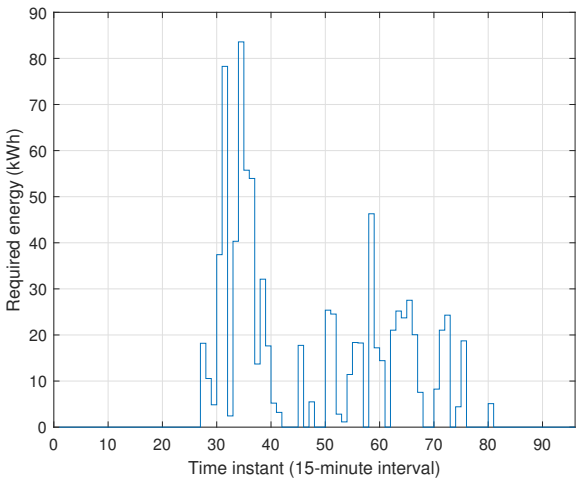

FIGURE 2. A typical charging energy demand profile on weekday at CSULB campus.

Considering that EV users may follow a consistent pattern in a short period, the week-ahead average number of charging requests at time instant h, denoted as $\overline{\gamma}(h)$, will be used as an estimation of the incoming EVs at h. Different from our previous work [32], the maximum number of charging requests is not considered, because such a conservative estimation may significantly reduce the profitability of charging services.

III. SOLUTION METHOD

In this section, Stage-II is conducted firstly to design and compare two charging power management approaches by fixing N, B, and P. The most computational efficient strategies will be selected and integrated with RSM to search for the optimal N, B, and P.

Let the decision time interval Δ to be 15-minute, aligning with the measurement time interval of solar power generation. This setting implies that accepted charging requests are consolidated within a 15-minute time frame and added to the service list. Subsequently, the power supply to each EV is updated at each 15-minute. Upon the arrival of an EV, its energy demand and desired charging period should be sent to the centralized decision-maker. When the expected waiting time has expired or the EV is fully charged, the charging cable can be disconnected, and the service request will be removed from the list. If no charger is available, new charging requests will be declined.

A. CHARGING MANAGEMENT SCHEME I

The model predictive control (MPC) based EV-charging management method was developed by authors in [32]. The current paper further integrates the BESS into the MPC formula, and replaces the worst-scenario estimation with the average number of service requests forecast. A simplified MPC framework is demonstrated in Fig. 3. At each sampling time step, a mathematical program is solved to allocate the charging power of each on-spot EV within the prediction horizon H. The management objective is to satisfy customers' requests and optimize revenue over the prediction horizon. Once the optimization solver determines the power sequence for EV at spot l, only the first charging action, denoted as $x_l(h|h)$, will be executed. This receding horizon manner adjusts future charging power based on the incoming information at each time step. Solving this optimization recurrently will generate the charging profile for each EV.

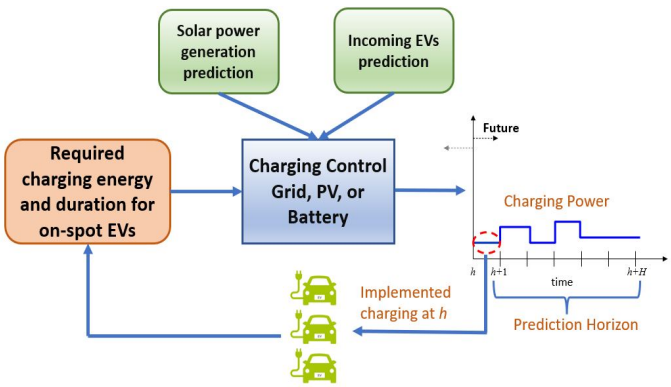

FIGURE 3. The overall structure of MPC based charging management.

The uncertain parameter of MPC is the solar power prediction $\hat{p}^g$ and number of incoming EVs. We assume that the 1-hour ahead prediction is accurate based on the weather data and the machine learning method proposed in [33]. If the prediction horizon H is longer than 1-hour, the monthly average solar power generation profile is used as a predictor. For the incoming EVs at h, the average number of charging requests $\overline{\gamma}(h)$ in the previous week is used as an estimation. Then, MPC is solved to optimize the H-step forecast revenue $\hat{\mathcal{R}}_H(h)$ at each time instant h:

$$\hat{\mathcal{R}}_H(h) = \max_{x,z,b} \Delta \sum_{k=0}^{H} \left(\sum_{l \in \Theta(h)} \alpha_C x_l(h+k|h) \right) \quad (\mathcal{MPC}1)$$

$$+\big(p^g(h+k|h)-p^c(h+k|h)\big)\alpha_{\mathrm{S}}+z(h+k|h)\cdot$$
$$\big(p^g(h+k|h)-p^c(h+k|h)\big)\big(\alpha_{\mathrm{B}}(h+k)-\alpha_{\mathrm{S}}\big)\Big)$$

$$\text{s.t. } p^c(h+k|h)=\sum_{l\in\Theta(h)}x_l(h+k|h)-b(h+k|h)$$
$$+Q\overline{\gamma}(h+w)\ \ \forall k\in[0,H], \tag{1a}$$

$$\beta(h)+\Delta\sum_{k=0}^{H}b(h+k|h)\leqslant B, \tag{1b}$$

$$(1-d_l(h+k|h))E+\Delta\sum_{k=0}^{H}x_l(h+k|h)\geqslant\eta_l(h),$$
$$\forall l\in\Theta(h),\ \forall k\in[0,H], \tag{1c}$$

$$d_l(h+k|h)\geqslant d_l(h+k-1|h),\ \forall l\in\Theta(h),\forall k\in[0,H], \tag{1d}$$

$$\nu(h)+\sum_{l\in\Theta(h)}d_l(h+k|h)-\sum_{w=0}^{k-1}\overline{\gamma}(h+w)\geqslant 0,$$
$$\forall l\in\Theta(h),\ \forall k\in[0,H], \tag{1e}$$

$$\Delta\sum_{k=0}^{T_l(h)}x_l(h+k|h)=\eta_l(h),\ \forall l\in\Theta(h)\text{ and }T_l(h)\leqslant H, \tag{1f}$$

$$\Delta\sum_{k=0}^{H}x_l(h+k|h)+Q\Delta(T_l(h)-H)\geqslant\eta_l(h),$$
$$\forall l\in\Theta(h)\text{ and }T_l(h)>H, \tag{1g}$$

$$p^g(h+k|h)-p^c(h+k|h)\leqslant(1-z(h+k|h))M,$$
$$\forall k\in[0,H], \tag{1h}$$

$$p^g(h+k|h)-p^c(h+k|h)\geqslant -z(h+k|h)M,$$
$$\forall k\in[0,H], \tag{1i}$$

$$z,d_l\in\{0,1\},\ 0\leqslant x_l\leqslant Q,\ |b(h)|\leqslant 0.2B, \tag{1j}$$

where set $\Theta(h)$ contains all occupied charging spots at time h; $b(h)$ is the battery charging/discharging power, bounded by 0.2 C-rate; binary variable z indicates whether solar power is greater or less than the power consumption; binary variable d_l indicates whether the EV at spot l completes its charging; $p^g(h)$ is the solar power generation at h; $p^c(h)$ is the total power consumption at h; parameter $\beta(h)$ represents remained energy in battery at h; parameter $\nu(h)$ is the number of empty chargers at the beginning of h; constant parameter E is the upper limit of EV energy demand; constant parameter M is the upper limit of solar power generation. For each on-spot EV, $\eta_l(h)$ and $T_l(h)$ are the required energy and allowable waiting time, respectively. These values, rather than state of charge (SOC), are recorded in our campus systems, and thus can be utilized in the charging management.

A series of discussions regarding ($\mathcal{MPC}1$) is shown below. The objective function is composed of three components: sales of solar power, charging fees, and grid power cost. Equation (1a) shows the total power consumption as a summation of the power charge of existing EVs, maximum power request of incoming cars, and battery power supply. Here if $b(h)>0$, then BESS discharges power to EV; otherwise, BESS is on charging. In addition, the battery cannot be charged beyond its capacity, as shown in (1b). Equation (1c) implies $d_l(h+k|h)=0$ before the supplied energy reaches demand $\eta_l(h)$. However, when total charging energy for EV at spot l is greater than $\eta_l(h)$ and more charging spots are needed, as shown in (1e), then $d_l(h+k|h)$ should be 1. Once $d_l=1$ at a time slot, then it implies that the task is completed and d_l should remain as 1 subsequently, as described in (1d).

If the permissible charging duration is less than the prediction horizon, (1f) necessitates the completion of charging tasks within the allowed time slots. If the permitted charging time exceeds the prediction horizon, then the maximum charging power Q kW is deployed out of the prediction horizon, as shown in (1g). Note that using the maximum power may not be the most economically efficient choice but ensures the shortest charging time. MPC with an infinite prediction horizon is theoretically sound. However, the long-term forecast error of solar power and serving requests, as well as increased computational demand make large H less attractive. Equations (1h) and (1i) determine if the solar power generation is greater or less than the power consumption.

In ($\mathcal{MPC}1$), the prediction process relies on average charging request numbers, with no consideration for predicting energy demands. Such uncertainty may lead to unnecessary delays in charging operations. Hence, we may further seek an alternative solution with the same operation revenue but maximizing the EV charging power while minimizing the battery charging or discharging rate at current time instant h. That formula is shown in ($\mathcal{MPC}2$):

$$\max_{x,z,b}\sum_{l\in\Theta(h)}x_l(h|h)-|b(h|h)| \tag{$\mathcal{MPC}2$}$$

$$\text{s.t. } (1a)-(1j), \tag{2a}$$

$$\hat{\mathcal{R}}_H^*(h)\leqslant\sum_{k=0}^{H}\Delta\Big(\sum_{l\in\Theta(h)}\alpha_{\mathrm{C}}x_l(h+k|h)+$$
$$+\big(p^g(h+k|h)-p^c(h+k|h)\big)\alpha_{\mathrm{S}}+z(h+k|k)\cdot$$
$$\big(p^g(h+k|h)-p^c(h+k|h)\big)\big(\alpha_{\mathrm{B}}(h+k)-\alpha_{\mathrm{S}}\big)\Big), \tag{2b}$$

where $\hat{\mathcal{R}}_H^*(h)$ is the optimal solution obtained from ($\mathcal{MPC}1$) at time instant h. The linear constraint (2b) guarantees that the profit yielded by ($\mathcal{MPC}2$) is the same with ($\mathcal{MPC}1$). The objective function maximizes the charging power at current time instant h and reduces the battery charging/discharging cycle. Using this formula, the charging schedule allows a charger to finish the existing services faster and accept more requests.

Formulas ($\mathcal{MPC}1$) and ($\mathcal{MPC}2$) are solved at each 15 minutes with updated $\Theta(h), T_l(h), \nu(h), \eta_l(h)$ and $p^g(h)$ for each EV. By summing the revenue at a single time slot, we can estimate the actual revenue $\mathcal{R}$ along the entire operating period. Station design parameters B and P have direct influence on the MPC solution. The available charging spots number N

does not explicitly exist in ($\mathcal{MPC}1$) and ($\mathcal{MPC}2$), but it impacts the total EVs that can be accommodated. Since each EV will be associated with a binary variable in the formula, the total service number will influence the online computational time. The bilinear term in the objective function of ($\mathcal{MPC}1$) can be equivalently converted to an auxiliary variable with a set of inequalities, as we have shown in [32]. Thus, the resulting formula ($\mathcal{MPC}1$) is an MILP, which can be solved to the global optimum. ($\mathcal{MPC}2$) is an MINLP due to the absolute value of $b(h|h)$ in the objective function. Note that MPC is relying on solar power prediction. Such uncertainties may significantly impact the performance of MPC.

B. CHARGING MANAGEMENT SCHEME II

This subsection proposes a new empirical rule method for charging management. Comparing with our preliminary results in [27], the new rule further integrates service prediction to optimize EV charging schedules. To make this paper self-contained, we provide the entire details of the charging rule. Let BESS be charged using solar power at no additional cost. During the energy peak time, the fully charged BESS becomes the power supply and curbs the energy drawn from the grid. Here we list the rule of battery charging/discharging:

- Starting from 6:00 AM, the BESS is charged and should be full before 4:00 PM, denoted as T_B.
- After 4:00 PM, the BESS-based EV charging gets priority.
- The BESS energy is solely used for EV charging rather than selling to the grid.

The charging period for BESS is determined by available solar energy resources. After 4:00 PM, α_G increases, and thus energy stored in the battery is preferred to use. Given that α_C is higher than α_S, the stored power should be used for EV instead of injecting back to the utility.

At step h, an EV at spot l should be charged at least by $\underline{x}_l$, and the battery should be charged at power $\underline{b}$:

$$\underline{x}_l(h) = \min\left\{Q, \max\{\eta_l(h)/\Delta - 7.2(T_l(h)-1), 0\}\right\} \quad (3)$$

$$\underline{b}(h) = \min\left\{0.2B, \max\{\beta(h)/\Delta - 0.2B(T_B-1), 0\}\right\} \quad (4)$$

The minimal charging power at h is calculated by using either Q kW or 0.2B charging rate in the subsequent time intervals. Furthermore, the following procedure is proposed to increase the scheduled minimal charging power for EVs based on the prediction of incoming service requests $\overline{\gamma}(h)$. This algorithm accelerates the charging process, and consequently reduces the number of rejected service requests.

Algorithm 1:
If $\overline{\gamma}(h) > \nu(h) + \sum_{l,T_l\leqslant 1} 1$, then
Step 1 $l' = \arg\min_{l\in\Pi(h)} \eta_l(h)$
Step 2 $\underline{x}_{l'}(h) = \eta_{l'}(h)/\Delta$
Step 3 $\Pi(h) \leftarrow \Pi(h) \setminus l'$ and $\overline{\gamma}(h) \leftarrow \overline{\gamma}(h) - 1$. If $\overline{\gamma}(h) > \nu(h) + \sum_{l,T_l\leqslant 1} 1$ and $\Pi(h) \neq \emptyset$, go back to step 1; else terminate algorithm.

where set $\Pi(h)$ is initialized as $\{l|T_l > 1 \text{ and } \eta_l(h) < Q\Delta\}$, representing EVs that can be charged to full at h but with longer allowable waiting time. Algorithm 1 is triggered when the number of expected incoming EVs is greater than the available charging spots.

Between 6 AM and 2 PM on weekdays or from 6 AM to 4 PM on weekends, the minimal power demands is initially fulfilled through PV and any deficit can be seamlessly supplemented by the grid. When there is surplus solar energy, priority is assigned to storing it in the battery or charging EVs. If neither EV nor BESS requires additional power, then the excess solar energy can be sold back to the grid.

- On weekdays from 6:00 AM to 2:00 PM or weekends from 6:00 AM to 4:00 PM, the minimal power $\underline{x}_l(h), \forall l \in \Theta(h)$ or $\underline{b}(h)$ is assigned to EV or battery.
- Then, if $p^g(h) > \sum_{l\in\Theta(h)} x_l(h) + b(h)$, we choose an EV l^* with the shortest permissible waiting time, denoted as $T_{l^*}(h)$. Let its charging power to be

$$x_{l^*}(h) = \max\left\{\underline{x}_{l^*}(h), \min\{Q, p^g(h) - \sum_{l\neq l^*} \underline{x}_l(h) - b(h), \eta_{l^*}(h)/\Delta\}\right\} \quad (5)$$

- If BESS has the most urgent charging need, and excess solar energy is available, then

$$b(h) = \max\left\{\underline{b}(h), \min\{0.2B, p^g(h) - \sum_{l} \underline{x}_l(h), \beta(h)/\Delta\}\right\} \quad (6)$$

Repeat the above procedure for each EV and BESS until the generated solar energy is exhausted.

$\eta_{l^*}(h)/\Delta$ or $\beta(h)/\Delta$ is integrated into the calculation to prevent overcharging. In the above algorithm, the charging power calculation starts from the minimal required power and gradually increases until solar power is fully utilized.

To minimize peak time charging on weekdays, we let EVs acquire the maximum possible solar energy before 4 PM. In addition, there is no need to postpone charging after 2 PM when solar energy resources begin to decline. The rule is

- On weekdays from 2:00 PM to 4:00 PM, there are:

$$x_l(h) = \min\left\{Q, \eta_l(h)/\Delta, \min\{T_l(h), 65-h\}\right\} \quad (7)$$

$$b(h) = \min\left\{0.2B, \beta(h)/\Delta(65-h)\right\} \quad (8)$$

There two formulas for $x_l(h)$ and $b(h)$ try to finish charging tasks before 4 PM, with the power bound Q kW or $0.2B$.

In peak hours, it is essential to minimize the charging tasks' power requirements to facilitate load shifting to off-peak periods. Furthermore, the non-grid power source is denoted as $p^{g'}(h) = p^g(h) + \min\{0.2B, \beta(h)/\Delta\}$.

- From 4:00 PM to 9:00 PM, the charging power is tentatively set as its minimal value $\underline{x}_l(h), \forall l \in \Theta(h)$.

- If $p^{g'}(h) > \sum_{l\in\Theta(h)} x_l(h)$, then we choose an EV l^* featured by the shortest allowable charging time, denoted as $T_{l^*}(h)$, whose charging power is

$$x_{l^*}(h) = \max\Big\{\min\{Q, p^{g'}(h) - \sum_{l\neq l^*} \underline{x}_l(h), \eta_{l^*}(h)/\Delta\}, \underline{x}_{l^*}(h)\Big\}. \tag{9}$$

  Repeat the above procedure and update the stored battery energy until $p^{g'}$ is used up or there is no remained charging request.
- The discharge rate of BESS is:

$$b(h) = -\min\Big\{\frac{\beta(h)}{\Delta}, 0.2B, \max\{\sum_{l\in\Theta(h)} x_l(h) - p^g(h), 0\}\Big\}. \tag{10}$$

In the evening, the power supply can be assigned to each time step evenly due to unchanged grid electricity price $\alpha_G(h)$. If an EV needs to depart later than the sunrise, its charging task is properly postponed to make use of more solar power. We use T_l' to denote the allowed charging time period after 6 PM. If an EV at spot l prefers leaving before 6 PM, then $T_l' = 0$.

- From 9:00 PM to 6:00 AM, there is:

$$x_l(h) = \min\Big\{Q, \max\{0, \frac{\eta_l(h) - Q\Delta T_l'}{\Delta \min\{T_l(h), T_{h\to 6}\}}\}\Big\}, \tag{11}$$

  where $T_{h\to 6}$ is the duration from current time point h to 6 AM.
- The discharging rate of BESS from 9:00 PM to 6:00 AM:

$$b(h) = -\min\{\frac{\beta(h)}{\Delta}, 0.2B, \sum_{l\in\Theta(h)} x_l(h)\} \tag{12}$$

Compared to the MPC approach, the empirical rule based method manages charging power without using solar power prediction and optimization solvers, and thus it offers agility in making charging decisions at the cost of losing some optimality. The principle of rule-based method is to maximize the utilization of available solar power, meet charging time constraint, and allocate enough charging spots for anticipated incoming cars. It is worthwhile to note that California benefits from relatively rich solar power resources, and the charging peak hour is consistent due to the fixed school course arrangement. The presented empirical rule thus is suitable.

C. INFRASTRUCTURE OPTIMIZATION

The RSM is a data-driven approach to determine the infrastructure parameters, P, N, and B. While MPC heavily depends on computationally-intensive optimization and receding horizon methods to adapt operations dynamically during the simulation, the rule based method without real-time optimization is more computationally efficient. Our simulation shows that the time consumption of rule-based versus MPC is nearly 1:67 (see Table 6). Given the rule-based charging revenue generated under many sampled designs, we can build a response surface model, which is used to search for a new optimal design solution. The new design and its neighbors will be sampled with shrinking level distance to evaluate and improve the surface function. This algorithm will be terminated when the searching level distance is shrunk to a low level. In addition, once the design is finalized, we can use MPC instead of the empirical rule for real operations. Comparing with preliminary results [27], the battery degradation is integrated within the RSM framework to characterize the total profit more accurately. We demonstrate the RSM flowchart in Fig. 4 and each step is discussed below.

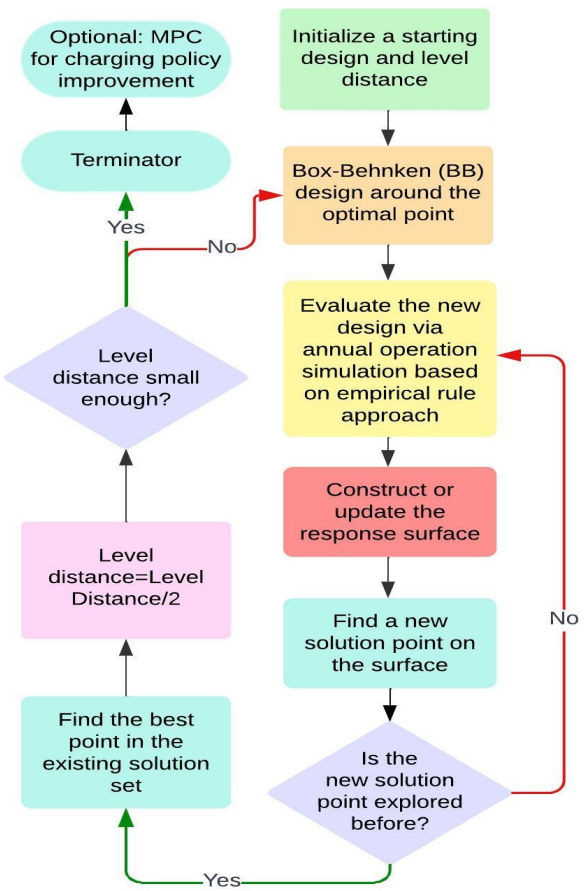

FIGURE 4. RSM algorithm flowchart. The rule-based approach is used to evaluate each design. Once the station design is finalized, the MPC can be applied to improve charging operations.

Sampling: According to reference [13], the 3-factor BB design only needs to evaluate 13 samples around the central sampling point. The changing direction for B, N, and P are represented by L_B, L_N, and L_P, respectively. Their values can be 1, 0, or -1. Assume that the current optimal design parameters are B^*, N^*, P^*. The level distances at this solution point are denoted as λ_{B^*}, λ_{N^*}, and λ_{P^*}, respectively. Then, the sampled solutions enumerated around the previous optimum

are:

$$B = L_B\lambda_{B^*} + B^*,\ N = L_N\lambda_{N^*} + N^*,\ P = L_P\lambda_{P^*} + P^*. \tag{13}$$

Design evaluation: The annual operational revenue can be quickly generated by the empirical rule method. The one-time infrastructure cost includes charger, BESS, and PV panel. The Level 2 charger cost per plug depends on the output power, denoted as α_N. We follow [38] to use the cost $\$6,000$, $\$6,500$, and $\$10,500$ for 7.2, 11, and 22 kW chargers, respectively. The battery price $\alpha_B(B)$ has already been shown in Table 1. The cost of a commercial solar carport panel stands at $\$1.56$ per Watt DC (WDC) in the U.S. market as of 2021, with an additional yearly maintenance cost of $\$17$ per KW [34]. Hence, the profit spanning for 10 years is:

$$\begin{aligned}\mathcal{P}(B,N,P) = &\sum_{j=0}^{9}\tilde{\mathcal{R}}(B(1-4j\%),N,P)\\ &-\alpha_B(B)-\alpha_N N-(1560+17\times 10)P,\end{aligned} \tag{14}$$

where $\tilde{\mathcal{R}}$ is the estimated operational revenue by taking battery degradation into account. The lithium iron phosphate battery under 0.5 C-rate usually degrades to 80% capacity after 6,000-8,000 cycles [35]. The manufacturer guarantees that its battery capacity at most reduces to 60% after 10-year. Thus, the annual capacity degradation of battery is assumed to be a constant 4%. This capacity degradation will adversely impact the operations of BESS and thus the profitability of charging station.

Construct and update surface function: Given the sampled designs and their revenue $\mathcal{R}$ evaluated by the annual operation simulation using empirical rule charging approach, a second-order surface function for estimated revenue can be defined in (15):

$$\begin{aligned}\tilde{\mathcal{R}}(B,N,P) =& c_0 + c_bB + c_NN + c_PP + c_{B2}B^2 + c_{N2}N^2\\ &+ c_{P2}P^2 + c_{BN}BN + c_{BP}BP + c_{NP}NP,\end{aligned} \tag{15}$$

where $c_0, c_b, c_N, c_P, c_{B2}, c_{N2}, c_{P2}, c_{BN}, c_{BP}$, and c_{NP} are model parameters identified through least squares. Then, $\tilde{\mathcal{R}}(B(1-4j\%),N,P)$ in (14) can be estimated through the following formula:

$$\begin{aligned}\tilde{\mathcal{R}}(B(1-4j\%),N,P) = &\mathcal{R} - c_b4j\%B - c_{BN}4j\%BN\\ &- c_{BP}4j\%BP - c_{B2}(1-(1-4j\%)^2)B^2\end{aligned} \tag{16}$$

As more samples are evaluated, the surface function can be updated by re-fitting the data.

Search a new design: The design solution can be updated by searching on the function $\mathcal{P}$ defined in (14).

$$\max_{B,P,N}\mathcal{P}(B,N,P) \tag{17}$$

The resulting optimization is an integer quadratic program, solvable by many off-the-shelf solvers.

Re-sampling: As shown in Fig. 4, if the solution derived from (17) has been explored before, then the best solution within the existing sampling set will be selected. Associated level distance of that solution is halved and BB-design re-samples new points within a smaller region around the selected solution. When the level distance of a solution point is small enough, it implies that the optimum is found.

Improve the charging: MPC is not integrated with RSM for infrastructure design because it takes much longer time than the rule-based method to determine the charging power for each EV. However, MPC is able to achieve higher operational profit due to its optimization nature. Therefore, we can use it to improve the charging strategy when the infrastructure is determined via RSM.

IV. SIMULATION

We conduct the simulation on a workstation with Intel Xeon Silver 4208 processor and 16 GB memory. The software platform is GAMS 41 with MILP solver CPLEX and MINLP/MIQP solver SCIP [36]. The termination condition for both CPLEX and SCIP is the relative gap 0.1% or solving time 200 seconds. The compared approach, adaptive particle swarm optimization (PSO) [37] is also programmed in GAMS.

A. INFRASTRUCTURE DESIGN

In the simulation study, the rule-based charging management is applied in the RSM for infrastructure design because MPC with a moderate prediction horizon $H = 15$ may take several hours to determine the annual operations even for one design solution. In contrast, the empirical rule approach completes the same task for about 10 minutes. The real world data introduced in Section II are used for simulation. After determining the optimal size and capacity of station infrastructure through RSM, we can still use MPC to further improve the charging policy and revenue. The goal is to determine the optimal number of chargers, the capacity of battery, and the size of solar panels, under various Level 2 charging power, including 7.2, 11, and 22 kW.

The BESS price $\alpha_B(B)$ is listed in Table 1. The TOU-EV-8 made by the utility company Southern California Edison (SCE) is shown in Table 2.

TABLE 1. Price of battery $\alpha_B(B)$ [28]

Capacity (kWh)	Price ($)
4	2,885
8	4,985
12	7,085
16	9,185
20	11,285
24	13,385
28	15,485
32	17,585
36	19,685
40	21,785
44	23,885
48	25,985
52	28,085

An initial guess of searching area on the surface function is shown in (18). Here B should be the capacity value in Table 1.

TABLE 2. Grid TOU price α_G [29]

Period	October-May	June-September
8 am-4 pm	\$0.10 /kWh	\$0.12 /kWh
4 pm-9 pm	\$0.23 /kWh	\$0.28 /kWh
9 pm-8 am	\$0.12 /kWh	\$0.12 /kWh

N and P can be any integer values in (18). If an optimal design is found on any boundary of (18) during RSM iterations, then the BB-design formula (13) will enable us to dynamically extend the searching area.

$$B \in [0, 52],\ N \in [10, 45],\ P \in [60, 250] \tag{18}$$

Table 3 shows the first set of sampled BB-designs and associated annual operational revenue with 7.2 kW chargers using the empirical rule based charging method. In addition, the analysis of variance (ANOVA) is conducted to investigate how three design variables impact the operational revenue. The resulting near-zero p-value indicates that all three design variables have substantial influences on revenue, and it is therefore advisable to optimize them concurrently.

TABLE 3. The first BB-design set:revenue with ANOVA using 7.2 kW chargers

$\mathcal{R}$	B	P	N
56847.913	12	100	32
68887.703	12	240	32
58110.644	52	100	32
70235.631	52	240	32
60699.234	12	170	20
64050.193	12	170	44
61975.569	52	170	20
65406.131	52	170	44
53825.395	32	100	20
58298.684	32	100	44
67215.242	32	240	20
69983.293	32	240	44
64464.340	32	170	32
F-value	12.10	1062.24	99.41
p-value	0.0078	0	0

Figs. 5-7 plot the profit of each sampled design solution during RSM iterations for 7.2, 11, and 22 kW chargers, respectively. Moreover, Figs. 8-10 show the sampled battery size, PV capacity, and number of chargers during RSM iterations for 7.2, 11, and 22 kW chargers, respectively. The initial 13 samples are distributed sparsely to explore different areas, and thus the resulting profits vary significantly. With more iterations, the samples are more concentrated, and the profit profiles in Figs. 5-7 become smoother. We terminate RSM when the level distance of B , P, and N reaches 4, 2, and 1, respectively. Figs. 11-13 frame the 3-dimensional (3D) solution space and color the profit for 7.2, 11, and 22 kW chargers, respectively. The RSM initially explores a wide range of design space, but quickly converges and generates more samples around a small high-profit area. The optimal solutions and resulting profits are shown in Table 4. Among three types of chargers, the 11 kW is preferred whose high profitability is due to a good balance between charging speed and capital cost. The solutions also show that larger PV-panels or BESS diminishes the overall profit due to the extended payback period resulting from the high initial capital investment. The BESS effectively shifts some of the solar power generated during the day to peak hours after sunset, which increases operational revenue. However, the high cost and capacity fading issue of BESS may degrade its merits.

We employ the adaptive PSO to solve the same design problem for comparison. Totally 13 independent particles are initialized at the same positions with BB-design of RSM. These particles can evolve with 13 generations, resulting in 169 evaluations, which is the same as the maximum evaluation number of RSM. Due to the stochastic nature, we execute the adaptive PSO with 5 different trials. The optimization results are shown in Table 5. Comparing it with Table4, we can see that the RSM outperforms PSO in all scenarios and trials. More importantly, the proposed RSM is a deterministic approach that does not require multiple trials.

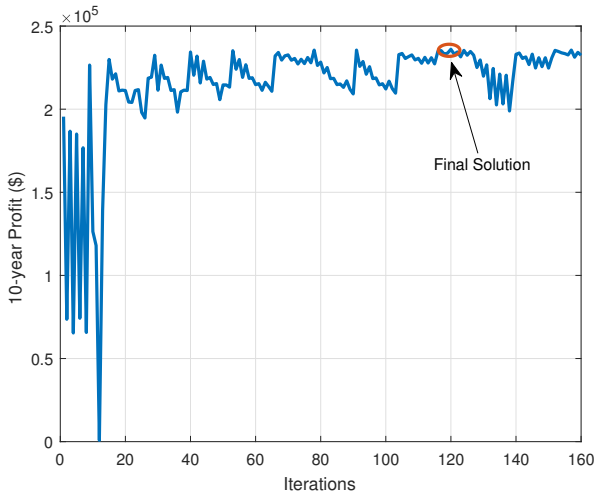

FIGURE 5. The profit evolution in RSM (7.2 kW charger).

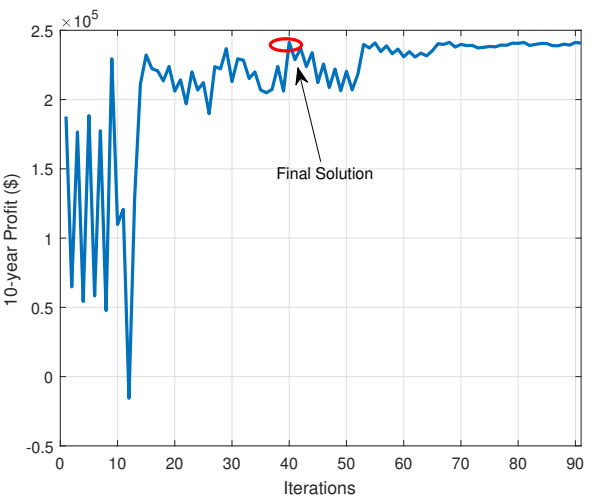

FIGURE 6. The profit evolution in RSM (11 kW charger).

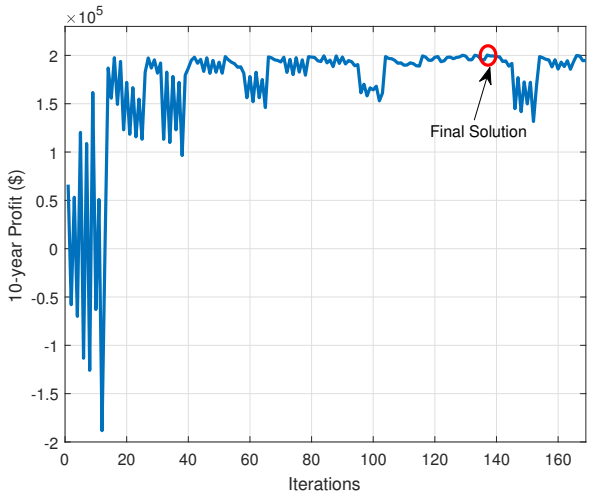

FIGURE 7. The profit evolution in RSM (22 kW charger).

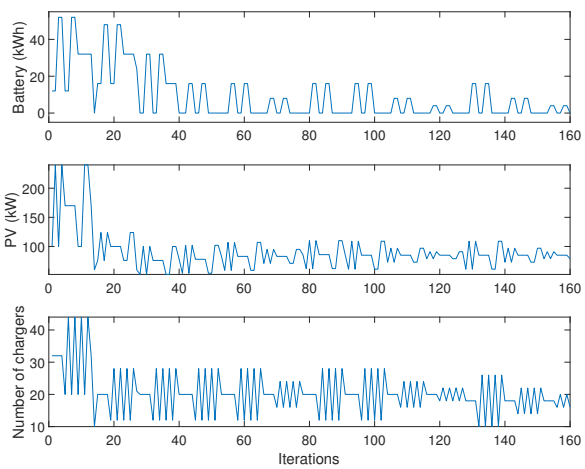

FIGURE 8. The enumerated design solutions in RSM (7.2 kW charger).

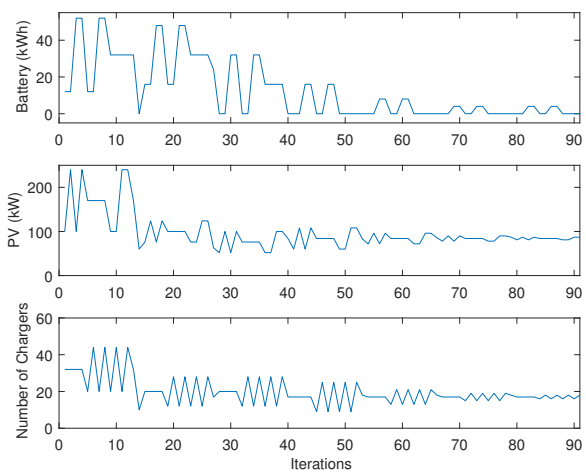

FIGURE 9. The enumerated design solutions in RSM (11 kW charger).

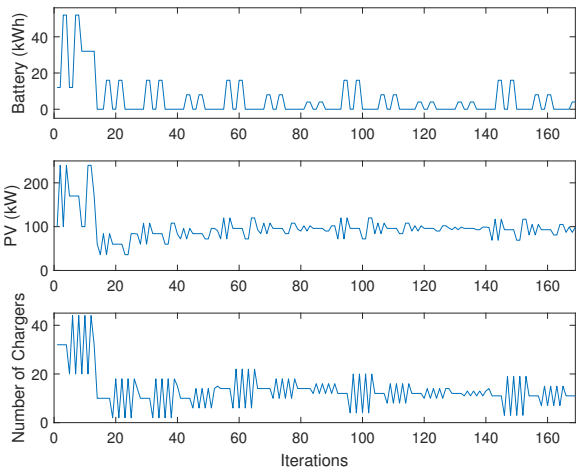

FIGURE 10. The enumerated design solutions in RSM (22 kW charger).

TABLE 4. Optimal solutions of the RSM

Charging Power (kW)	B	P	N	10-year Profit ($)
7.2	0	85	18	236028
11	0	84	17	241352
22	0	93	11	200328

After creating the response surface for operational revenues $\mathcal{R}$, we use the 7.2 kW case as an example to gradually reduce the BESS cost and investigate when BESS is preferred. The optimal solution in Table 6 shows that BESS becomes attractive when its market price $\alpha_B(B)$ is halved. It is not supervised because utility incentives for surplus solar energy offset the advantage of BESS.

B. CHARGING MANAGEMENT

Apart from the rule-based charging management, we set $H = 15$ and execute MPC to operate the charging station under the same design parameters for comparison. Here only the 7.2 kW charger is applied as an example presented in Table 6.

TABLE 5. Optimal solutions of adaptive PSO

Charging Power (kW)	Trials Number	B	P	N	10-year Profit ($)
7.2	1	0	86	21	234668
7.2	2	0	78	18	235188
7.2	3	0	96	18	233739
7.2	4	0	88	19	235753
7.2	5	0	94	19	234976
11	1	4	87	19	238214
11	2	16	94	16	237055
11	3	0	95	18	240708
11	4	12	91	17	238437
11	5	4	90	18	239354
22	1	0	89	13	198684
22	2	16	88	11	196415
22	3	0	79	13	197329
22	4	0	92	12	200294
22	5	0	95	13	199582

We observe that MPC requires significantly more time to optimize the annual operation due to the need of solving ($\mathcal{MPC}1$) and ($\mathcal{MPC}2$) at each time instant. It demonstrates that a long prediction horizon significantly increases the MPC's solving time. Regarding the operational revenue and declined services in two scenarios, MPC is superior to the rule-based method because of its real-time optimization nature. Moreover, this finding contradicts with our preliminary result in [27] because the incoming car prediction is newly integrated within both MPC and rule-based approaches. However, the high computational demands of MPC hinders its integration with the RSM for infrastructure optimization. When a battery is deployed in the charging station, MPC must decide whether battery, solar, or grid power is used. This additional task renders the MPC to spend more computational time. The simple charging rule with incoming car number prediction needs much less time without solving optimization, and generates only 8% lower revenue than that of the MPC. Considering that RSM needs to evaluate the annual operations under 160 different designs shown in Fig. 5, a simple charging rule method is more suitable to the RSM-based infrastructure design. Once the station design parameters are fully determined, then MPC can be used to manage the charging power of each EV.

The annual charging power profiles using MPC and rule-based approach at all $3657 \times 24 \times 4 = 35040$ time instants are plotted in Fig. 14. More power is needed during January to March because of spring semester course schedule whereas less power is demanded during the summer break. Because rule-based approach heavily relies on solar power to charge EVs, it accepts a smaller number of services and thus requests less power. To better illustrate this, we further plot Fig. 15 for one-day EV charging profiles using MPC-based and rule-based strategies, respectively. The rule-based approach aligns EV charging with solar power generation before 4:00 PM to optimize cost, while MPC is more aggressive to acquire more charging power from the grid and accommodate a larger amount of charging demands. For example, at 27^{th} time instant (6:45 AM), only two charging requests with expected waiting time 9.75 and 5.25 hours are received. At that time instant, the rule-based method only provides the charging power 0.1438 kW due to the lack of solar power, whereas MPC charges EVs using grid power supply with 14.4 kW.

To test the function of BESS in EV charging, we halve the battery price and find that deploying a 12 kWh BESS in the charging station is profitable. The one-day battery charging/discharging operations using rule-based approach and MPC under 0.2-C rate are shown in Fig 16, respectively. The rule-based method treats BESS as a long-term charging request in the morning and starts charging at 11 AM when solar power is high enough. The BESS becomes full before 4 PM. After 4 PM, the BESS discharges to supply EV power. The MPC determines BESS operations by solving two optimization problems at each time instant. It stops charging the battery before 4 PM even though it may not be full, and discharges it to supply EV power demands in the evening.

Finally, we need to acknowledge the limitations inherent

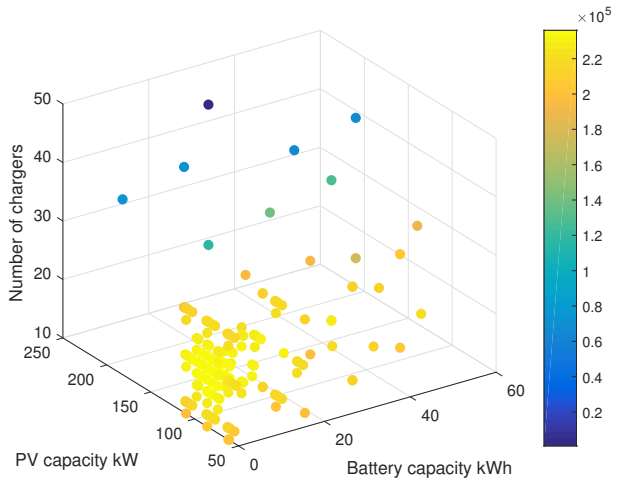

FIGURE 11. **The sampled design parameters in 3D space and their 10-year profit (7.2 kW charger). Color: Profit**

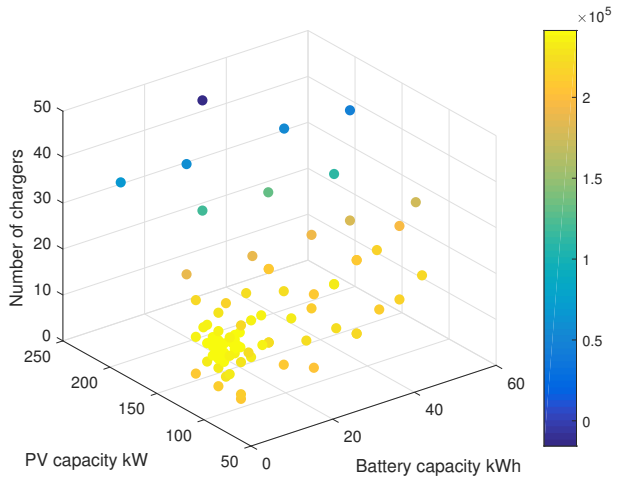

FIGURE 12. **The sampled design parameters in 3D space and their 10-year profit (11 kW charger). Color: Profit**

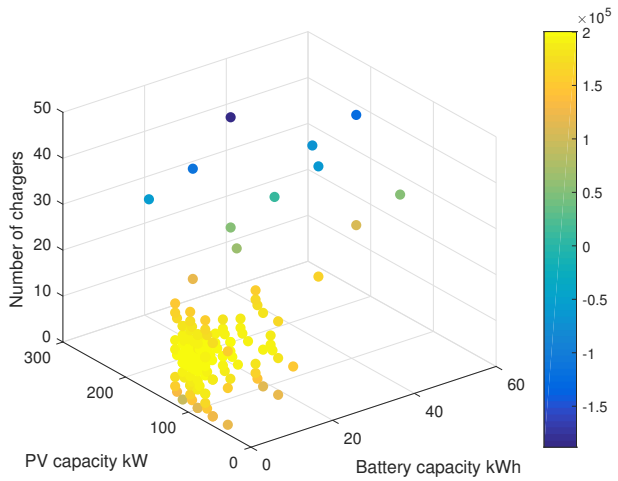

FIGURE 13. **The sampled design parameters in 3D space and their 10-year profit (22 kW charger). Color: Profit**

TABLE 6. One-year Operational Revenue, Simulation Time for Single Design, and Declined Services under the Optimal Solutions. Note: Two optimal designs are generated. BESS is employed in the second solution when $\alpha_B(B)$ is halved. 7.2 kW charger is applied.

Design (B: 0 P: 85 N: 18)	Rule	MPC
$\mathcal{R}(\$)$	49107.89	53000.85
Simulation Time (minutes)	9.7	648.3
Declined Service	2289	774
Design (B: 12 P: 86 N: 20)	Rule	MPC
$\mathcal{R}(\$)$	50928.18	53852.61
Simulation Time (minutes)	11.9	6000.3
Declined Service	1856	582

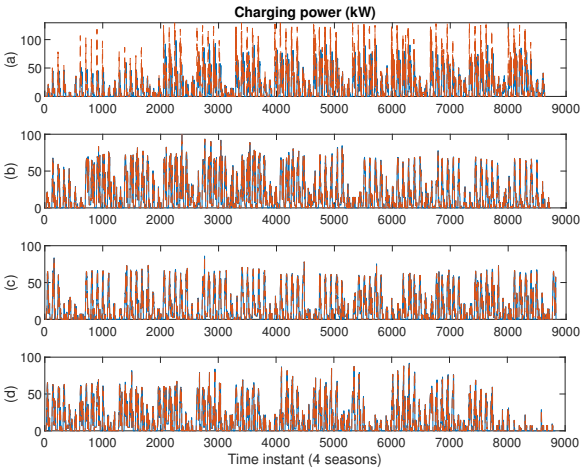

FIGURE 14. Annual charging power using MPC and rules-based approaches, 7.2 kW chargers. Blue solid: Rule-based; Red dash: MPC; (a) Jan.-Mar. (b) Apr.-Jun. (c) Jul.-Sep. (d) Oct.-Dec.

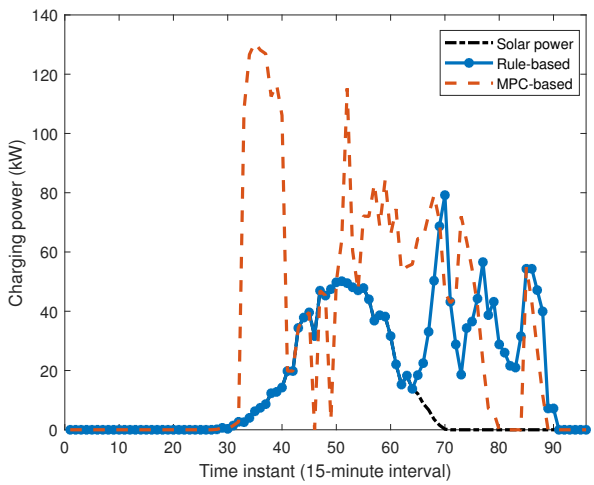

FIGURE 15. One-day EV charging and solar power generation (B=0, P=85, N=18), 7.2 kW chargers. MPC: Acquires more power from grid for EV charging. Rule-based: Aligns with solar power generation before peak hour (4:00 PM).

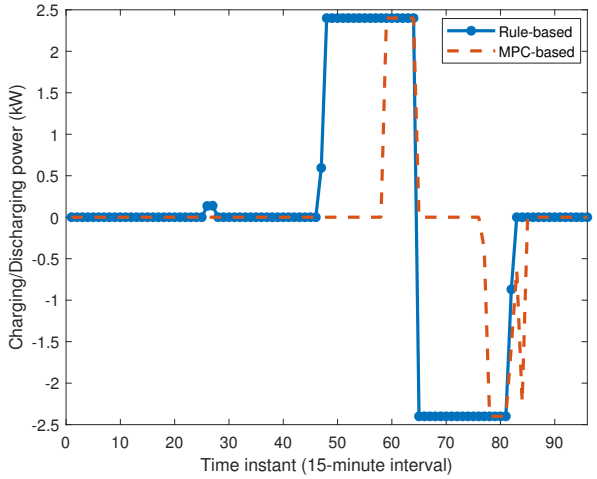

FIGURE 16. One-day battery operations (B=12, P=86, N=20), 7.2 kW chargers. MPC: BESS is not full before peak hour (4:00 PM). Rule-based: BESS is full before peak hour (4:00 PM).

in the proposed design and management approaches. Our study is confined to a 3D searching space with quadratic surface function. However, for higher-dimensional design space, a more complex surface function becomes necessary. In addition, how to reduce the performance gap between the empirical rule based charging method and MPC still deserves more investigations.

V. CONCLUSION

Our study introduces a comprehensive framework aimed at achieving a near-optimal design of a PV and BESS-assisted charging station. We develop two distinct charging management approaches, MPC and the rule-based method. MPC, leveraging solar power and charging request predictions, solves two optimization problems to determine the optimal charging solution at each time step. In contrast, the empirical rule predominantly utilizes solar power in daytime charging and shifts loads to the off-peak hours. This rule relies on the charging request forecast without engaging with optimization, and thus resulting nearly 1/67th of the computation time required by MPC. We then develop the RSM to optimize the design solution by maximizing long-term profit with the rule-based charging schedule instead of MPC due to its computational efficiency. The one-year charging requests collected on the station and solar power data are used for simulation to assess the presented scheme. The proposed charging rule yields slightly less revenue compared to the MPC, but substantially reduces solving time, making it particularly suitable for implementation within RSM to explore the design space effectively. Furthermore, the RSM-based analysis shows that the high-price BESS subject to capacity degradation is unfavorable to the charging station profitability when excess solar energy can be sent back to the utility with incentives. In fact, the BESS is preferred only when its price is halved. In addition, we compare the deterministic RSM with a stochastic optimization method, adaptive PSO, and demon-

strate that RSM consistently achieves better solutions in all tested scenarios. This comprehensive evaluation underscores the robustness and efficiency of our proposed framework for designing and managing PV and BESS-assisted charging stations.

ACKNOWLEDGMENT

Authors appreciate the CSULB Parking & Transportation Department for providing data.

REFERENCES

[1] M. Alexander, N. Crisostomo, W. Krell, J. Lu, and R. Ramesh, "Assembly Bill 2127 Electric Vehicle Charging Infrastructure Assessment (Revised Staff Report)," *California Energy Commission*, 2021.

[2] S. Habib, M. M. Khan, F. Abbas, L. Sang, M. U. Shahid, and H. Tang, "A comprehensive study of implemented international standards, technical challenges, impacts and prospects for electric vehicles," *IEEE Access*, vol. 6, pp. 13866-13890, 2018.

[3] H. G. Yeh, S. Sim, and R. Bravo, "Wavelet and denoising techniques for real-time HIF detection in 12 kV distribution circuits," *IEEE Systems J*. vol 13. pp. 4365-4373, 2019.

[4] H. G. Yeh, D. H. Tran, and R. Yinger, "High impedance fault detection using orthogonal transforms," Proc. IEEE Green Energy and Systems Conference, Long Beach, CA, Nov. pp. 67-72, 2014.

[5] H. Chen, Z. Hu, H. Luo, J. Qin, R. Rajagopal, and H. Zhang, "Design and planning of a multiple-charger multiple-port charging system for PEV charging station," *IEEE Transactions on Smart Grid*, vol. 10, pp. 173-183, 2019.

[6] Y. Li and J. Wu, "Optimum integration of solar energy with battery energy storage systems," *IEEE Transactions on Engineering Management*, vol. 69, no.3, pp. 697-707, 2022.

[7] S. Negarestani, M. Fotuhi-Firuzabad, M. Rastegar, and A. Rajabi-Ghahnavieh, "Optimal sizing of storage system in a fast charging station for plug-in hybrid electric vehicles," *IEEE Transactions on Transportation Electrification*, vol. 2, no.4, pp. 443-453, 2016.

[8] P. Mirhoseini and N. Ghaffarzadeh, "Economic battery sizing and power dispatch in a grid-connected charging station using convex method," *Journal of Energy Storage*, vol. 31, 101651, 2020.

[9] O. Ekren, C. H. Canbaz, and C. B. Güvel, "Sizing of a solar-wind hybrid electric vehicle charging station by using HOMER software," *Journal of Cleaner Production*, vol. 279, pp. 123615, 2021.

[10] M. H. Moradi, M. Abedini, S. M. R. Tousi, S. M. Hosseinian, "Optimal siting and sizing of renewable energy sources and charging stations simultaneously based on Differential Evolution algorithm," *Electrical Power and Energy Systems*, vol. 73, pp. 1015-1024, 2015.

[11] M. R. Mozafar, M. H. Moradi, M. H. Amini, "A simultaneous approach for optimal allocation of renewable energy sources and electric vehicle charging stations in smart grids based on improved GAPSO algorithm," *Sustainable Cities and Society*, vol. 32, pp. 627-637, 2017.

[12] J. Li, S. He, Q. Yang, T. Ma, and Z. Wei, "Optimal design of the EV charging station with retired battery systems against charging demand uncertainty," *IEEE Transactions on Industrial Informatics*, vol. 19, pp. 3262-3273, 2023.

[13] G. Box and D. Behnken, "Some new three level designs for the study of quantitative variables," *Technometrics*, vol. 2, pp. 455–475, 1960.

[14] A. S, Al-Ogaili, T. J. T. Hashim, N. A. Rahmat, A. K. Ramasamy, M. B. Marsadek, M. Faisal, and M. A. Hannan, "Review on scheduling, clustering, and forecasting strategies for controlling electric vehicle charging: challenges and recommendations," *IEEE Access*, vol. 7, pp. 128353-128371, 2019.

[15] S. Limmer, "Evaluation of Optimization-Based EV Charging Scheduling with Load Limit in a Realistic Scenario," *Energies*, vol. 12, no. 24, pp. 4730, 2019.

[16] Y. He, B. Venkatesh, and L. Guan, "Optimal scheduling for charging and discharging of electric vehicles," *IEEE Transactions on Smart Grid*, vol. 3, no. 3, pp. 1095-1105, 2012.

[17] M. E. Kabir, C. Assi, M. H. K. Tushar, and J. Yan, "Optimal scheduling of EV charging at a solar power-based charging station," *IEEE Systems Journal*, vol. 14, no. 3, pp. 4221-4231, 2020.

[18] W. Tushar; C. Yuen; S. Huang; D. B. Smith; H. V. Poor, "Cost minimization of charging stations With Photovoltaics: An approach with EV classification," *IEEE Transactions on Intelligent Transportation Systems*, vol. 17, no.1, pp. 156-169, 2016.

[19] T. Zhang, W. Chen, Z. Han, and Z. Cao, "Charging scheduling of electric vehicles with local renewable energy under uncertain electric vehicle arrival and grid power price," *IEEE Transactions on Vehicular Technology*, vol. 63, no. 6, pp. 2600-2612, 2014.

[20] H. Li, Z. Wan, and H. He, "Constrained EV charging scheduling based on safe deep reinforcement learning," *IEEE Transactions on Smart Grid*, vol. 11, no. 3, pp. 2427-2439, 2020.

[21] D. Yan, H. Yin, T. Li, and C. Ma, "A two-stage scheme for both power allocation and EV charging coordination in a grid-tied PV–Battery charging station," *IEEE Transactions on Industrial Informatics*, vol. 17, no. 10, pp. 3262-3273, 2021.

[22] R. Ghotge, Y. Snow, S. Farahani, Z. Lukszo, and A. Wijk, "Optimized scheduling of EV charging in solar parking lots for local peak reduction under EV demand uncertainty," *Energies*, vol. 13, no. 5, pp. 1275, 2020.

[23] Y. Zhang and L. Cai, "Dynamic charging scheduling for EV parking lots with photovoltaic power system," *IEEE Access*, vol. 6, pp. 56995-57005, 2018.

[24] Maigha and C. L. Crow, "Cost-constrained dynamic optimal electric vehicle charging," *IEEE Transactions on Sustainable Energy*, vol. 8, no. 2, pp. 716-724, 2017.

[25] Y. Zheng, Y. Song, D. J. Hill, and K. Meng, "Online distributed MPC-based optimal scheduling for EV charging stations in distribution systems," *IEEE Transactions on Industrial Informatics*, vol. 15, no. 2, pp. 638-649, 2019.

[26] L. Bartolucci, S. Cordiner, V. Mulone, M. Santarelli, F. Ortenzi F, and M. Pasquali, "PV assisted electric vehicle charging station considering the integration of stationary first- or second-life battery storage," *Journal of Cleaner Production*. 2023;383:135426.

[27] Y. Yang and H. Yeh, "Electrical Vehicle Charging Infrastructure Design and Operations," *Mineta ransportation Institute Publications*. 2023.

[28] "Lithium Batteries," https://www.ecodirect.com/Lithium-Batteries-s/1080.htm (accessed Nov. 10, 2022)

[29] "Southern California Edison Rate," https://www.sce.com/regulatory/tariff-books/rate-change (accessed Nov 10, 2022)

[30] "Net Surplus Compensation Rate," https://www.sce.com/regulatory/tariff-books/rates-pricing-choices/net-surplus-compensation (accessed Nov. 10, 2022)

[31] "California Distributed Generation Statistics," https://www.californiadgstats.ca.gov/downloads (accessed Nov. 10, 2022)

[32] Y. Yang, H. G. Yeh, and R. Nguyen, "A robust model predictive control-based scheduling approach for electric vehicle charging with photovoltaic systems," *IEEE Systems Journal*, vol. 17, pp. 111-121, 2023.

[33] Y. Yang, J. Mao, R. Nguyen, A. Tohmeh, and H.G. Yeh, "Feature construction and selection for PV solar power modeling," 2022 IEEE International Symposium on Advanced Control of Industrial Processes (AdCONIP), pp. 90-95, 2022.

[34] V. Ramasamy, D. Feldman, J. Desai, and R. Margolis, "U.S. solar photovoltaic system and energy storage cost benchmarks: Q1 2021," Technical Report: NREL/TP-7A40-80694, National Renewable Energy Lab.(NREL), Golden, CO (United States), 2021.

[35] Y. Preger, H. M. Barkholtz, A. Fresquez, D. L. Campbell, B. W. Juba, J. Romàn-Kustas, S. R. Ferreira, and B. Chalamala, "Degradation of commercial lithium-ion cells as a function of chemistry and cycling conditions," *Journal of The Electrochemical Society*, vol. 167, pp. 120532, 2020.

[36] T. Achterberg, "SCIP: solving constraint integer programs," *Math. Prog. Comp.*, vol. 1, pp. 1-41, 2009.

[37] Z. Zhan, J. Zhang, Y. Li, and H. S. Chung, "Adaptive particle swarm optimization," *IEEE Transactions on Systems, Man, and Cybernetics-Part B: Cybernetics*, vol. 39, pp. 1362-1381, 2009.

[38] B. Borlaug, S. Salisbury, M. Gerdes, and M. Muratori, "Levelized cost of charging electric vehicles in the United States," *Joule*, vol. 4, pp. 1470-1485, 2020.

YU YANG received the B.S. degree from Beijing Institute of Technology, Beijing, China, in 2004, the M.S. degree from Zhejiang University, Hangzhou, China, in 2007, and the Ph.D. degree from the Department of Chemical Engineering, University of Alberta, Edmonton, Canada in 2011. He then became a postdoctoral associate at the Massachusetts Institute of Technology. He currently is an associate professor in the Department of Chemical Engineering, California State University Long Beach. His research interests include the data-driven modeling, advanced process control, machine learning, and global optimization of energy systems.

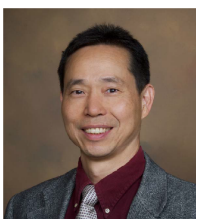

HEN-GEUL YEH (SM'82) received the B.S. degree in engineering science from National Chen Kung University, Taiwan, ROC, in 1978, and the M.S. degree in mechanical engineering and the Ph.D. degree in electrical engineering from the University of California, Irvine, in 1979 and 1982, respectively. Since 1983, he has been with the Electrical Engineering department at California State University, Long Beach (CSULB), USA, and served as the department Chair since 2016. In addition to his technical and engineering excellence, he was selected as a NASA JPL Summer Faculty Fellow twice, in 1992 and 2003, respectively, and the Boeing Welliver Faculty Fellow in 2006. His research interests include DSP/Communication/Control algorithms development using MATLAB, and implementation using FPGA and digital signal processors with applications to communication systems, smart grids, optimization, controls, and electrical event detection, with focus on real-time Digital Signal Processing, Wi-Fi and Wi-MAX, adaptive systems, and mobile communication in multipath fading channels. He has published more than 100 research papers on Signal Processing, Communications, Controls, and Smart Grids. Dr. Yeh is a professional engineer in Electrical and is the recipient of five NASA Tech. Brief and New Technology awards from the National Aeronautics and Space Administration (NASA), the inventor's award and other awards at the Aerospace Corporation, the Northrop Grumman Excellence in Teaching award, College of Engineering, CSULB, 2007, the Distinguished Faculty Scholarly and Creative Achievement Award, CSULB, 2009 and Outstanding Professor Award, CSULB, 2015. He has received four US patents in the area of Signal Processing, Communication and Controls, Since 2010, he has served as the organizer and Conference Chair of IEEE Green Energy and Smart Systems Conference (IGESSC).

NGUYEN CAM THUY DAM was a student at California State University, Long Beach, since 2020, after receiving an Associate degree in Science and Mathematics from Fullerton College. She received a B.S. degree in Chemical Engineering with a minor in Chemistry in the Fall of 2022 semester. Dam is interested in researching the application of automatic control in the chemical engineering field, renewable energy, development of chemical process design, simulation, and optimization.